



ELSEVIER

Contents lists available at ScienceDirect

Additive Manufacturing

journal homepage: www.elsevier.com/locate/addma

Research Paper

Feature-based characterisation of Ti6Al4V electron beam powder bed fusion surfaces fabricated at different surface orientations

Lewis Newton^{a,*}, Nicola Senin^{a,b}, Evangelos Chatzivagiannis^c, Bethan Smith^c, Richard Leach^a^a Manufacturing Metrology Team, Faculty of Engineering, University of Nottingham, UK^b Department of Engineering, University of Perugia, Italy^c Manufacturing Technology Centre, Coventry, UK

ARTICLE INFO

Keywords:

Metrology

Surface topography

Surface texture

Feature based characterisation

ABSTRACT

Due to the layer-based nature of the powder bed fusion (PBF) process, part surfaces oriented in space at varying angles with respect to the build direction are differently affected by a wide array of manufacturing-induced phenomena (staircase effects, spatter, particles, etc.), which can significantly influence the functional behaviour of such surfaces, and choices for post-processing where needed. For assessing surface topography of PBF surfaces most researchers have looked at surface texture parameters (profile - ISO 4287 and areal - ISO 25178-2). Texture parameters provide useful summaries of surface-wide properties, but do not allow the analysis to focus on specific topographic formations of interest. On the contrary, feature-based characterisation encompasses a series of recently introduced methods that allow to isolate and characterise specific topographic formations of interest starting from topography datasets acquired with conventional areal topography measurement solutions. In this work, the topography of electron beam powder bed fusion (EBPBF) surfaces as a function of orientation with respect to the build direction was investigated using a combined approach consisting of both texture parameters and feature-based characterisation. A custom-designed test part featuring surfaces at different orientations was measured with a focus variation instrument. A feature-based characterisation pipeline was implemented for the identification, isolation and geometrical characterisation of spatter formations and particles present on the as-built surfaces. The surfaces deprived of the identified features were then characterised by means of conventional ISO 25178-2 texture parameters. The results confirm that combining feature-based characterisation with conventional analysis through texture parameters creates new perspectives for looking at EBPBF surfaces, thus better supporting future research endeavours aimed at achieving a more comprehensive insight on the nature of EBPBF surfaces. For the first time quantitative results are provided on number, shape and localisation of spatter and other particles in EBPBF surfaces as a function of build orientation, and texture parameters are provided that describe the fabricated surfaces in a more reliable way as particles and spatter formations have been removed.

1. Introduction

For layer-based additive manufacturing processes such as powder bed fusion (PBF) a build direction can be identified as the vector perpendicular to the imaginary plane where the layer fabrication process takes place. In PBF processes, the build direction is typically vertical and corresponds to the direction along which the part grows, layer after layer. The surfaces of a part being fabricated by PBF will usually lay at various orientations with respect to the build direction, and orientation significantly influences many of the geometric and topographical properties of such surfaces. For example, in PBF, the topography of a horizontal surface will correspond to the topography of the last layer

fabricated for it. On the contrary a surface that is tilted with respect to the horizontal plane will contain the outer edges of multiple layers, staggered apart to produce what commonly known as the staircase effect [1,2]. Other sources for topographic variability caused by surface orientation are the irregularities of the physical bonding between the fused layers, particularly visible in vertical or almost vertical surfaces [3] and the presence of different amounts of particles or spatter attached to the surface [1,4,5]. The capability to predict surface topography in relation to orientation offers awareness of the challenges one will need to overcome when designing post-processing tasks needed to make the part compliant to design specifications (e.g. finishing operations by machining).

* Corresponding author.

E-mail address: lewis.newton@nottingham.ac.uk (L. Newton).<https://doi.org/10.1016/j.addma.2020.101273>

Received 15 November 2019; Received in revised form 26 March 2020; Accepted 19 April 2020

Available online 18 May 2020

2214-8604/ Crown Copyright © 2020 Published by Elsevier B.V. This is an open access article under the CC BY license (<http://creativecommons.org/licenses/by/4.0/>).

Most of the research investigating surface texture in powder bed fusion has focused on laser processing (i.e. laser powder bed fusion - LPBF). In this work, we focus on electron beam powder bed fusion (EBPBF). EBPBF is conceptually similar to LPBF in terms of how the process operates (a layer is produced by raster scanning a powder bed with a point energy source in order to induce local melting) but produces surfaces whose topographies are rather different from laser powder bed fusion [6]. The main differences found in EBPBF relate to the scanning strategy used to produce the layers, which involves three subsequent scans: a) heating of the whole bed, b) melting of internal regions of the part through hatch scanning, and c) melting of the contour [6]. As a result of the initial heating step, EBPBF parts are embedded in a sintered powder, or 'part cake', which further interacts with the other bonding mechanisms requiring some intensive mechanical removal after the manufacturing process is complete.

Experimental investigation of surface topography of LPBF parts as a function of surface orientation has been commonly carried out by using custom test parts (artefacts) designed to possess surfaces at different orientations with respect to the build direction [7]. The assessment of topographic differences across surfaces has been frequently carried out by computing ISO 4287 profile texture parameters [8]. The most commonly used parameter is R_a , the arithmetic mean deviation of the assessed profile [9–11]. However, because of the complex nature of most AM topographies, characterisation based on individual profiles may often fail to capture significant aspects [7]. On the contrary, areal measurement can provide richer information content, and related texture parameters, referred to as areal parameters and defined within ISO 25178–2 [12], have been found to provide more relevant insight on additive topographies [7]. Despite their recognised advantages, areal texture parameters have been used far less often. The most commonly adopted areal parameters have been: S_a , the arithmetic mean height of the scale-limited surface (the areal equivalent to R_a) and S_q , the root mean square height of the scale limited surface (the areal equivalent to R_q – the root mean square deviation of the assessed profile) [13–16].

The advantage of using texture parameters (whether profile or areal based) is that complex topography information can be summarised by a reduced set of scalar values (the values of the parameters), thus allowing for very easy quantitative comparison between surfaces. The disadvantage of texture parameters is that they are designed to capture widespread properties that characterise the entire measured region, for example the overall amount of "roughness", intended as unorganised scatter of height values above and below a reference mean plane, (which incidentally is what is described by the aforementioned parameters R_a , S_a and S_q). Surface texture parameters cannot highlight the presence of singularities or perform any spatial decomposition of the surface in order to focus on sub-regions that may be more informative in terms of explaining the manufacturing process. For example, surface texture parameters would not be able to describe how many particles are present on a surface, or what is their spatial distribution or whether they exhibit a tendency to form clusters over the measured region. Because of these limitations, feature-based characterisation of topography has been recently proposed as an alternative to texture parameters [17]. In feature-based characterisation, topography is spatially decomposed into regions (segmentation), each encapsulating a local topographic formation bearing any conceptual relevance in the specific application. Each region (referred to as feature) is then individually characterised in terms of its geometric properties (size, shape, localisation, etc.) and (if needed) localised with respect to other features/objects, thus leading to a topological network of relevant features present on the surface. Feature-based approaches have been recently investigated for the characterisation of laser powder bed fusion surfaces [5,18–21]: in these works, digital topographies obtained by measurement have been partitioned to isolate objects such as weld tracks, spatter formations, unmelted particles and other topographical features that are typical of LPBF processes, thus providing quantitative data useful for researchers to investigate the events that lead to the

generation of such features during the manufacturing process. The disadvantage of feature-based characterisation is that topography decomposition and feature isolation/description pipelines must be carefully designed and fine-tuned for every test case, since topographies (and thus partitioning needs) differ across applications, and characterisation objectives may require focusing on different geometrical properties of the features [17].

This work introduces two main elements of novelty: a) the feature-based decomposition of EBPBF surfaces is investigated for the first time: whilst feature-based approaches have been proposed for LPBF [5,18], the different nature of EBPBF topographies requires new carefully tuned data analysis and processing pipelines [18] in particular for the isolation of the relevant features; b) a hybrid approach is proposed where part of the topographic formations (specifically, spatter and particles) are identified and separated via feature-based characterisation, whilst the underlying topography that has been devoid of these features is described through conventional surface texture parameters. The proposed hybrid approach is particularly relevant as a means to describe how the topography of EBPBF surfaces varies as a function of surface orientation with respect to the build direction: as stated earlier, particles (individual or in clusters) and spatter formations (on top surfaces) are typically present in varying amounts depending on surface orientation; as they are protruded, particles and spatter can influence significantly the computation of any areal field texture parameter, thus making the characterisation of the substrate surface often impossible. Because particles and spatter are typically welded to the substrate, even their mechanical removal does not produce a reliable surface for the computation of texture parameters because of the modification they leave behind in the regions they were attached to, thus a solution for masking particles and spatter out from the topography is preferable. In addition, being able to separate particles and spatter from their surroundings allows also for the selective computation of their geometrical and positional properties. Therefore, the separation of particles and spatter from the substrate enables the computation of particle number, size, spatial distribution, tendency to form aggregates, etc, which in turn leads to the possibility of describing surfaces as a function of orientation with respect to the build direction in a more informative and comprehensive way.

2. Methodology

2.1. Measurement test part

A 'Bracelet' test part made of Ti6Al4V ($91 \times 91 \times 30$) mm was manufactured using EBPBF with an Arcam A2 \times . The part features an external cylindrical surface (outer surface - Fig. 1.a) designed for the purpose of testing the method proposed in this paper. The surface is made of 36 planar facets with local orientation with respect to the build direction varying in 10° increments (0° , 10° , 20° , etc.). The orientation angle is measured from the horizontal plane (i.e. the virtual plane where each layer is fabricated, orthogonal to the actual build direction). So, a 0° -orientation surface is parallel to the horizontal plane, orthogonal to the part growth direction. Part geometry is shown as a CAD model in Fig. 1a. The z axis visible in the figure identifies the build direction, and points towards the direction of part growth. According to such coordinate system, the x,y plane is parallel to the virtual planes where each layer is fabricated and is therefore referred to as the 0° -orientation if the surface is facing upwards (180° if facing downwards). Surfaces with orientation = 90° are vertical, i.e. parallel to the build direction, whilst surfaces with orientation between 90° and 180° are downward facing, and part of overhanging regions. The fabrication of the test geometry by EBPBF requires support structures to handle the overhangs: the position of the supporting structures is shown in summary form in Fig. 1b by the added blue parts. The topography of downward facing surfaces is expected to be different because of (amongst other reasons) the presence of support structures in most

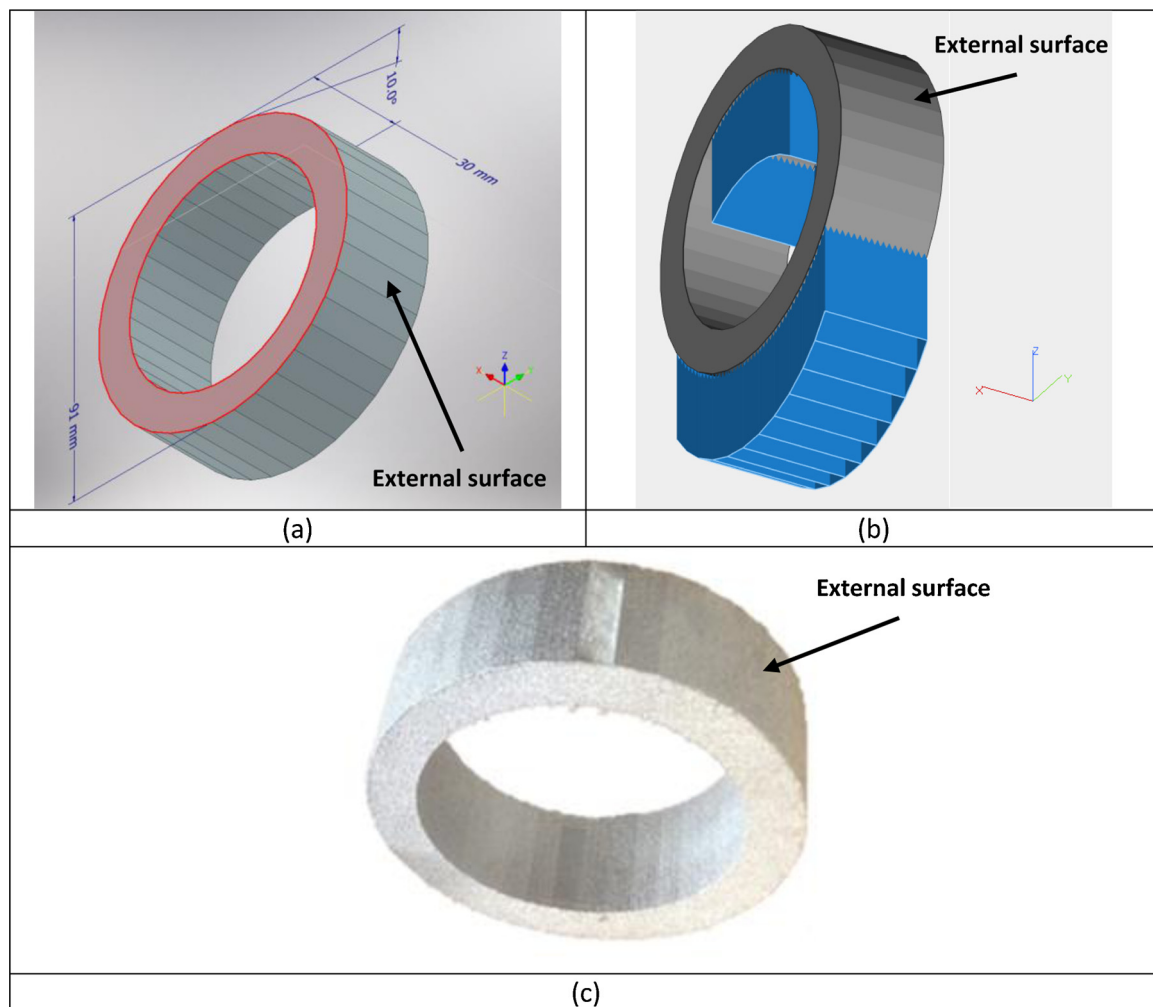


Fig. 1. 'Bracelet' test part: (a) CAD design; (b) support structures indicated in blue; (c) photograph of manufactured part.

cases, affecting surface topography, even after removal. The final produced test geometry is visible in Fig. 1c, where all the support structures were removed, and all the surfaces were cleaned using compressed air. Any further post-processing was ruled out because of the risk of removing meaningful, process-related features from the surfaces. In Fig. 1c, the 0° -oriented surface is the shiny one, visible at the top-centre of the bracelet geometry. It should be noted that due to the symmetry of the geometric design, surfaces placed to the left and right of the 0° -orientation top surface have the same absolute values in terms of orientation angle, but different sign (e.g. $\pm 10^\circ$). As these surfaces were found basically identical, topography was assumed as dependent on absolute orientation, but not sign of orientation angle, thus only one of the two surfaces available for each absolute orientation was studied (e.g. only the $+10^\circ$ surface).

2.2. Measurement strategy

Measurement was performed using an Alicona G5 focus variation (FV) areal topography measurement instrument [22]. Focus variation was demonstrated to be a suitable technology for the measurement of metal AM surfaces [23]. The following settings for the FV instrument were adopted: $20\times$ objective lens (NA 0.4; FoV (0.81×0.81) mm); lateral resolution: $3.51\ \mu\text{m}$; vertical resolution: 12 nm; ring light illumination; measured area (3×3) mm, stitched. Magnification and extents of the measured areas were chosen to capture a sufficiently representative portion of the surfaces, suitable both for the identification of a sizeable number of particles and spatter formations, and for the

characterisation of the underlying substrate via texture parameters.

Measurements were performed on the external surfaces over three regions for each individual facet placed at a different orientation in the test part, which are orientated in order to measure them flat in reference to the measurement system. Examples of measured topographies are shown in Fig. 2. In the figure, the measured raw datasets are reconstructed as triangle meshes and rendered in uniform colour using artificial illumination.

2.3. Feature-based segmentation

Particles and spatter formations were then identified by application of a segmentation method (i.e. spatial partitioning of the measured field) based on active contours, an edge detection method originally developed for image processing [24]. Details on the implementation of the method for surface topography can be found in [21]. However, a brief explanation is provided here to aid the illustration of the overall approach. The segmentation starts with an initial guess on the position of the features and their boundaries. From this guess, an iterative procedure is applied which increasingly refines the boundaries by narrowing or expansion, until a stable result is achieved, which supposedly corresponds more accurately to the real boundary of each feature of interest. Finally, the segmentation method proceeds to identify partitions delimited by such boundaries. If successful, some partitions will contain particles or spatter instances, others will contain the remaining topography (i.e. the surroundings). [24–28].

In this work, in order to create the initial mask for the active

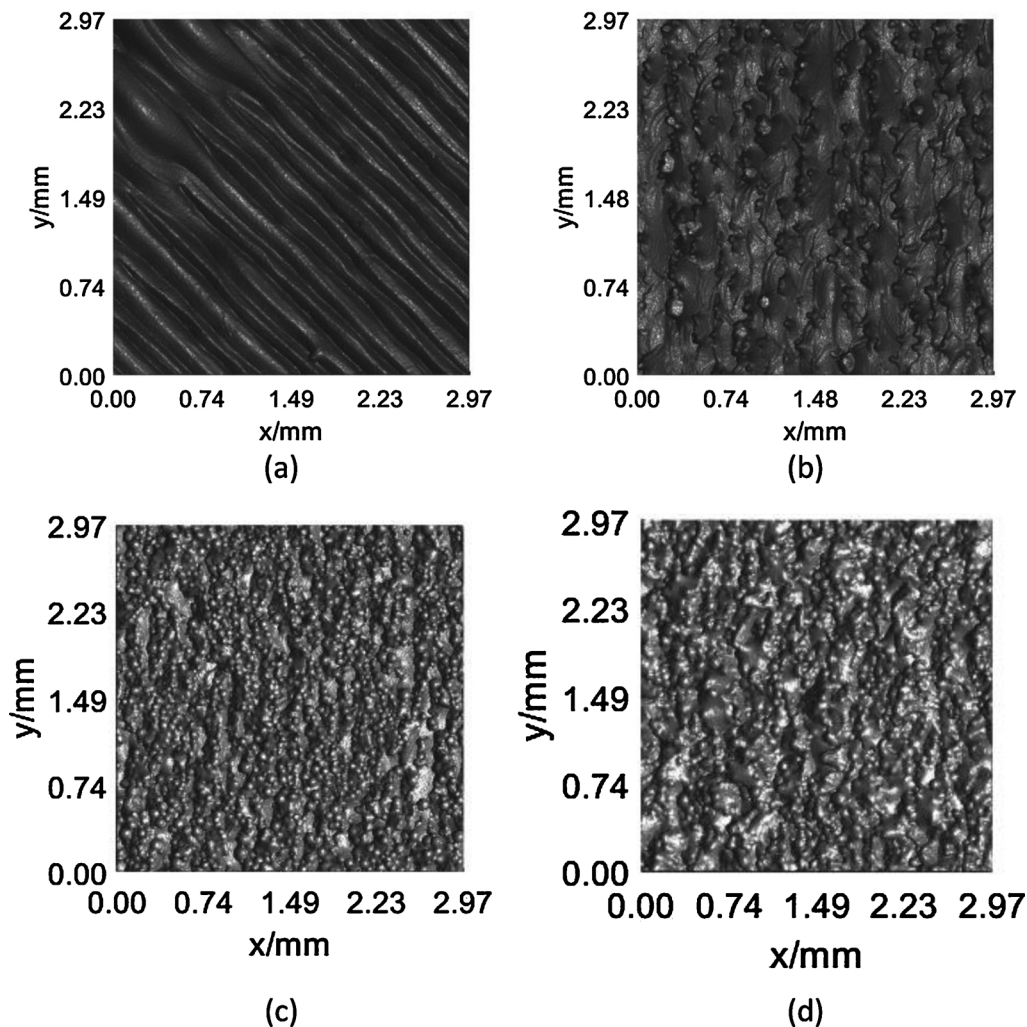


Fig. 2. Topography maps at varying surface orientation angle: (a) 0° (b) 30°, (c) 90°, and (d) 150°.

contours procedure, the surface topography was levelled by subtraction of the least-squares mean plane [29] (Fig. 3a), and subjected to filtering operations. Firstly, an S-filter to remove small-scale topographic formations (short spatial wavelengths) i.e. noise, was applied. The S-filter had a nesting index (i.e. cut-off wavelength) of 5 μm . Then an L-filter was applied to remove larger-scale topographic formations (i.e. long spatial wavelengths), i.e. any feature potentially larger than a particle or spatter formation. The L-filter had nesting index of 70 μm . The nesting indices for the S and L filters were the result of a series of preliminary filtering attempts, driven by the rationale that particles and spatter formations of sizes between 45 μm and 100 μm are typically found in EBPBF surfaces [30], and considering that filtering is implemented by convolution with Gaussian kernels (with 50 % transmission at the cut-off). On the topography resulting from filtering (Fig. 3b) a height thresholding operation was applied, meant to isolate the topmost regions of the filtered topography, most likely belonging to protruded formations such as spatter and particles (Fig. 3c). Thresholding was performed using different threshold values depending on surface orientation. On the resultant thresholded binary mask (= 1 for regions above the threshold, 0 for regions below), topologically disconnected isles were identified, then some were filtered out based on size, aspect-ratio and height (in the corresponding height map) not consistent with known geometric attributes of typical spatter formations and particles (Fig. 3d).

Boundaries extracted from the final isle mask were individually used as initial contour guesses for running the active contours

algorithm. Active contours was run over 100 iterations, using the geodesic active contours 'edge' method [25] with negative contraction bias (leading to outwards growth, i.e. the initial contour expands outwards from its initial shape). The active contours edge method updates the initially guessed contour by looking at the underlying height values in the topography and by locally displacing the contour towards the highest local gradients, corresponding to the steepest slopes. The final result of active contours was a segmentation mask containing contours closely matching the boundaries of the spatter/particle features in the original topography (Fig. 3e). A test for topological connectedness was finally used to isolate the mask regions occupied by each individual feature (Fig. 3f). Two important considerations must be made here: the first is that filtering is only used to temporarily alter the topography in order to facilitate the feature identification and isolation process (i.e. up to the point where the mask is obtained). Filtering is then rolled back, and the original topography is the one that gets processed using the mask, to separate features and surroundings. Features will be then processed with the original characterisation procedure described in Section 2.4, whilst the surroundings (in their original shape) will be processed through computation of texture parameters, as describe in Section 2.5.

2.4. Feature-based characterisation of surface topography

The topography regions containing the features, as indicated by the mask, were separated from the original topography and stored into a

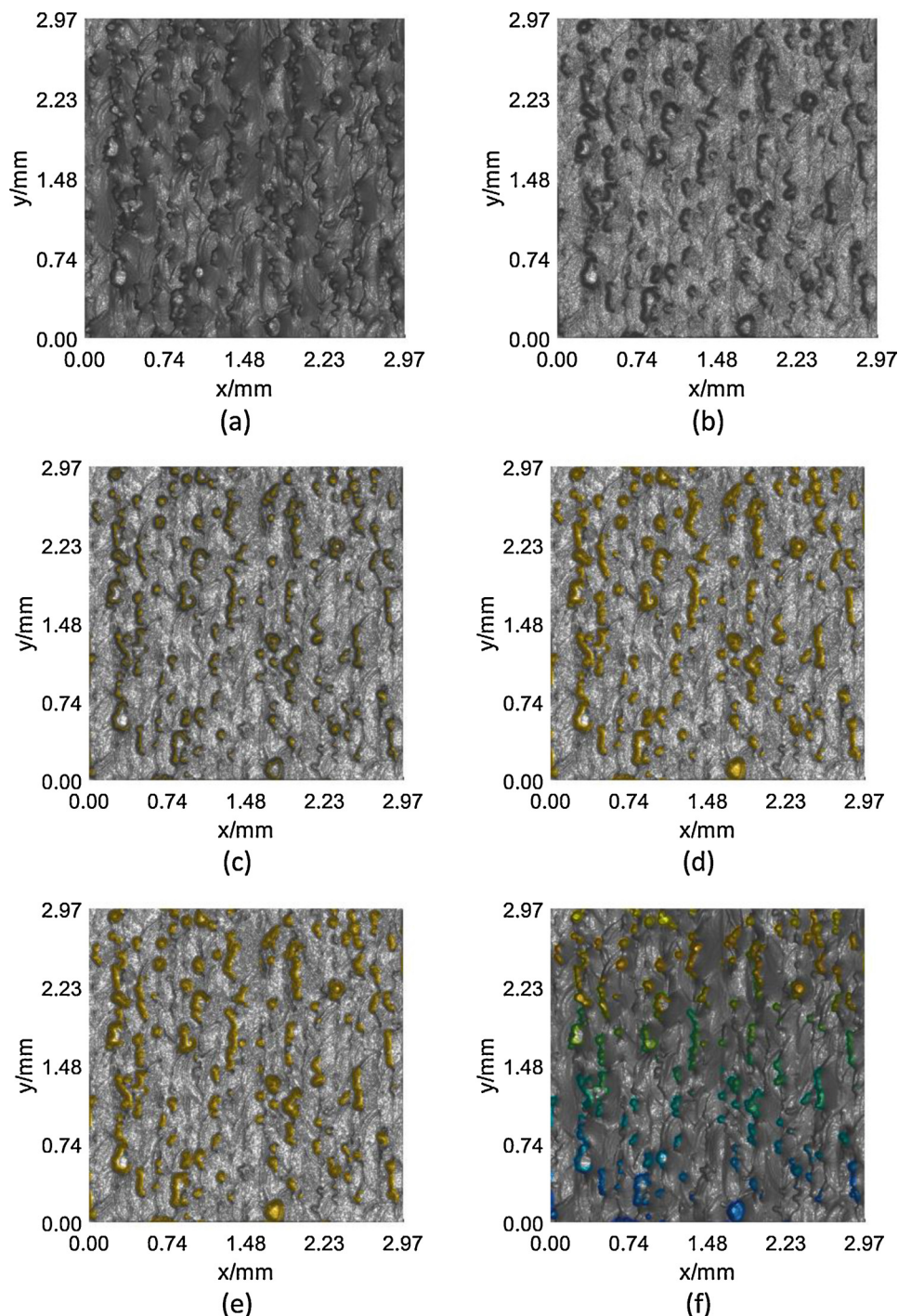


Fig. 3. Active contours segmentation approach, showing (a) original topography after levelling; (b) result of S and L filtering operation; (c) masked topography after height thresholding (yellow representing regions above the threshold, i.e. initial identification candidates); (d) masked topography after removal of incompatible candidates because of shape/size properties; (e) masked topography after active contours (yellow now representing the final identified features); and (f) original unfiltered topography with the identified features now shown in different colours (after separation by testing for topological connectedness).

new dataset (by voiding all the masked out height values). Each identified feature (Fig. 3f) was considered as belonging to the general class “particle/spatter”. A further discrimination to distinguish between spatter formations, individual particles, clusters of particles, or other unclassified protruded singularity would in theory be possible but was reserved for future work. The following quantitative indicators were defined:

- *feature count*: the number of features found on the surface. Obtained by counting the number of topologically disconnected isles in the final segmentation mask. Because of how the target feature has been

defined, it should be noted that a cluster of connected particles counts as 1;

- *feature area*: the areal footprint of each feature on the x,y plane. Obtained by counting the pixels enclosed within each isle of the segmentation mask, multiplied by pixel width information, available from measurement;

- *feature height*: the difference between the mean height of the topmost region of the feature, and the mean height of the region surrounding the feature (see Fig. 4). The topmost region of the feature is found by assessing the top 10 % heights as determined from a material

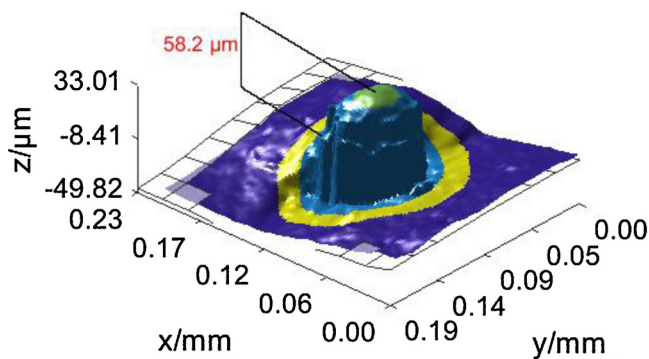


Fig. 4. Feature height indicator computed on a feature instance. The topmost region (green) and region surrounding the feature (yellow) are highlighted.

ratio curve plotted from the height values of the feature region. The region surrounding the feature is found by identifying the pixels mapped to the boundaries of the feature (i.e. the boundary pixels of each isle in the segmentation mask) and by applying an outwards-only dilation operation on the mask, up to 11 pixels (approximately $19.3 \mu\text{m}$) – corresponding to a wide enough region from which to compute a mean height around the feature itself. Importantly, feature height is computed on the topography dataset obtained after levelling (i.e. Fig. 3a, before any filtering is applied – the filtering shown in Fig. 3b was only used to facilitate segmentation).

- *feature coverage (%)*: the ratio of the sum of the feature areas (considering all the features identified within the measured area), divided by the total measured area, expressed as a percentage. This also considers features that are cropped by the borders of the measured region.

All the computations were performed on repeat measurements, so that boxplots for the feature-based quantitative indicators could be generated.

Following the computation of the indicators, all the identified instances of the targeted feature were removed from the original topography datasets by means of voiding the corresponding data points (i.e. labelling them as "non-measured"). An example of voided topography is shown in Fig. 5.

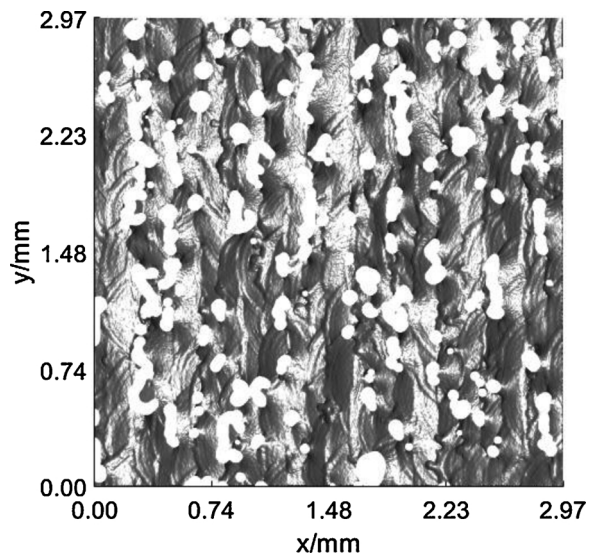


Fig. 5. Example topography after the identified particles/spatter formations have been removed (feature-deprived topography). This is an example of topography dataset which was used to compute texture parameters.

2.5. Characterisation based on computing ISO 25178–2 surface texture parameters

Texture parameters were computed both on the original surface topographies (i.e. as measured) and on those resulting from feature removal as described in the previous section (i.e. feature-deprived topographies). In both cases, computation of texture parameters was performed using the surface metrology software MountainsMap [31]. For computing texture parameters, the following operations were performed on the topography datasets: levelling by least squares mean plane subtraction; S-filter (noise removal) with cut-off wavelength 0.008 mm ; L-filter (waviness removal) with cut-off wavelength 0.25 mm . The same operations were applied to both the original topographies and the feature-deprived ones.

The following ISO 25178–2 areal texture parameters were calculated:

- Sa – arithmetic mean height of the scale-limited surface;
- Sq – root mean square height of the scale-limited surface;
- Ssk – skewness of the scale-limited surface;
- Sku – kurtosis of the scale-limited surface and
- Sz – maximum height of the scale limited surface.

All the computations were performed on repeat measurements, so that boxplots of texture parameter values could be generated to assess quantitative differences of results obtained for different surface orientations.

3. Results

3.1. Feature-based characterisation

As shown in Fig. 6, the number of features typically increases with larger surface orientation angles (recalling that 0° orientation corresponds to a horizontal, upward facing surface, 90° orientation corresponds to a vertical surface, and $> 90^\circ$ orientation corresponds to a downward facing surface). The 0° orientation surface (Fig. 6a) appears to mostly consist of weld tracks with very little presence of particles/spatter. In the 30° orientation surface (i.e. tilted but still facing upwards) (Fig. 6b) more particles/spatter formations are present. In addition, the staircase effect is sometimes mistaken as further particles/spatter by the method, because of its protruded nature. For angles close to 90° the topographies appear dominated by particles (Fig. 6c). Finally, in downwards oriented surfaces (e.g. Fig. 6d) an increment of what appears to be particle agglomeration is visible. This latter finding is consistent with a known phenomenon of powder bed fusion, where in downwards facing regions, because of the energy applied on the layers above, topographies are formed which are dominated by inter-layer bonding with the surrounding powder bed [32]. On the contrary, vertical surfaces are mostly subjected to partial melting and sintering of powder particles adjacent to the part, again consistent with what observed in Fig. 6b.

The values of the feature-related quantitative indicators defined in Section 2.4 were computed using individual, stitched measurements from three surface regions for each individual orientation in the test part. For the feature count indicator there was a total of three observations; for the feature height and feature area indicators the results were aggregated from all the identified features in the three regions on the same surface. Boxplots were used to present the median, interquartile range (IQR) and the range of data (either total range or that representing 95 % of the cases, in the latter case using circles to indicate outliers and crosses to indicate extreme outliers, which are greater than three times the IQR from the end of the box). The interquartile range is a measure of the difference between the lower and upper quartile values (which represent 25 % and 75 % of the data respectively).

The results for the feature count indicator (the number of identified features) are shown in Fig. 7. Feature count increases with build angle (as visually confirmed in Fig. 6). Between the 60° to 110° orientations

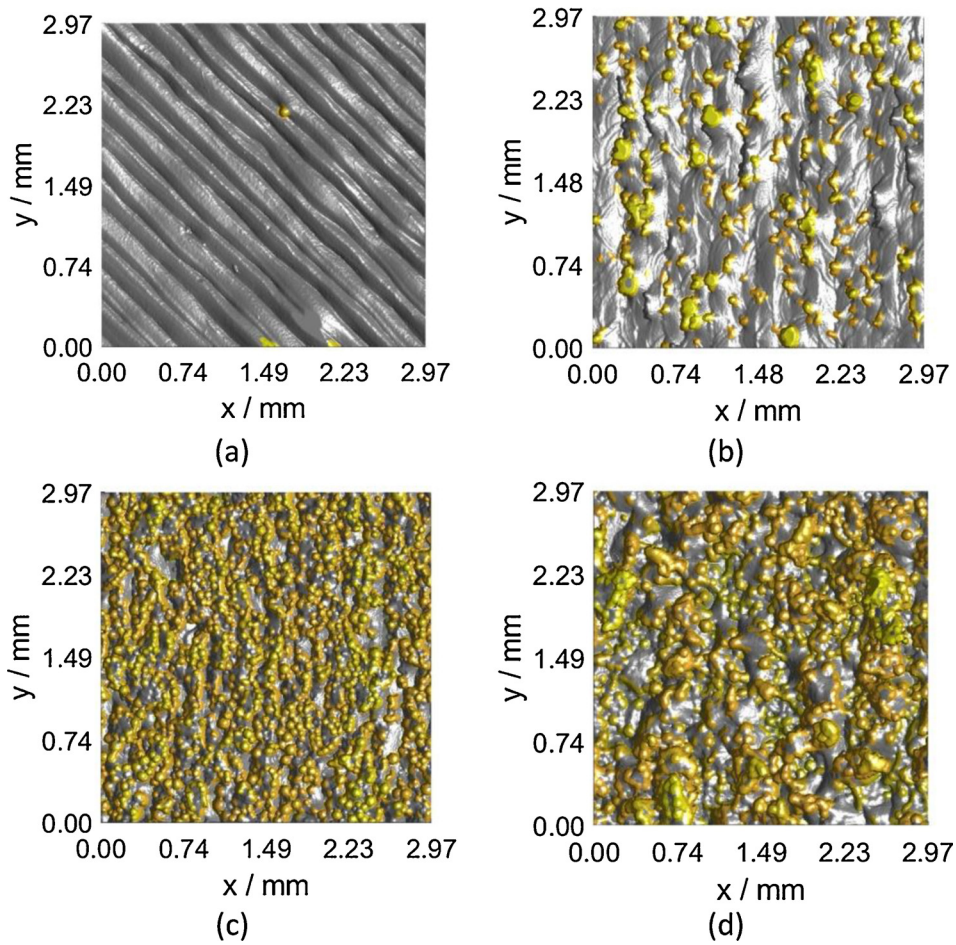


Fig. 6. Example feature identification results; (a) 0° orientation, (b) 30° orientation, (c) 90° orientation, and (d) 120° orientation (downward facing surface).

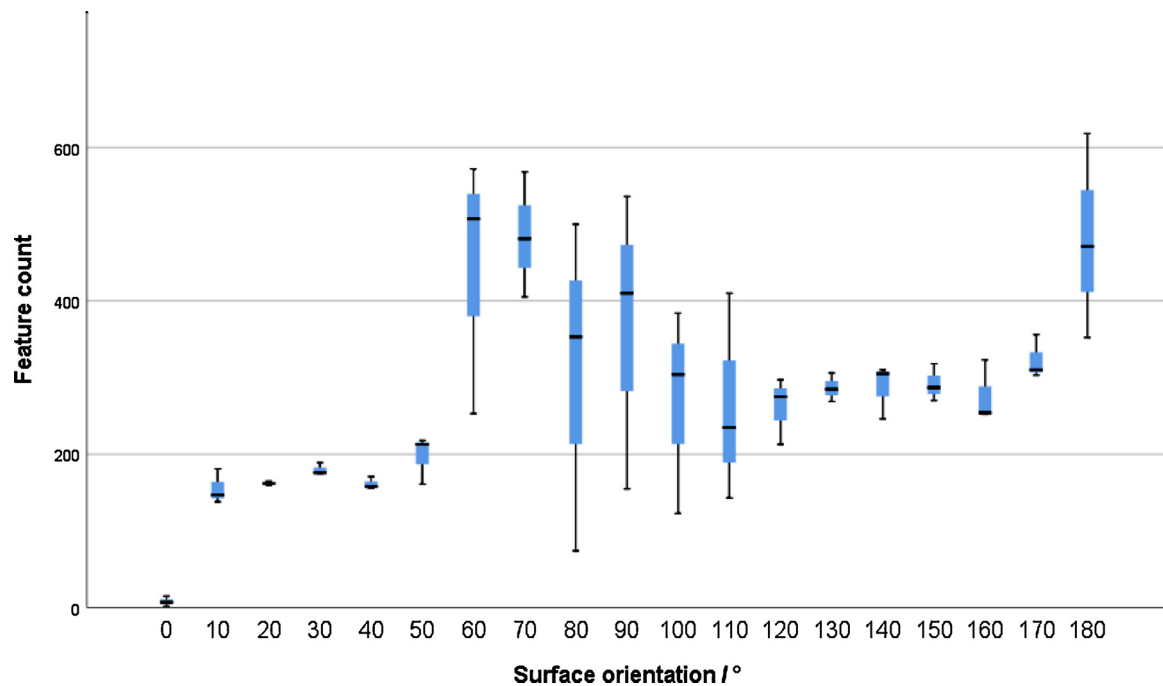


Fig. 7. Feature count (number of individual features) as a function of surface orientation. Median, interquartile range (IQR) and whiskers (the range) are shown.

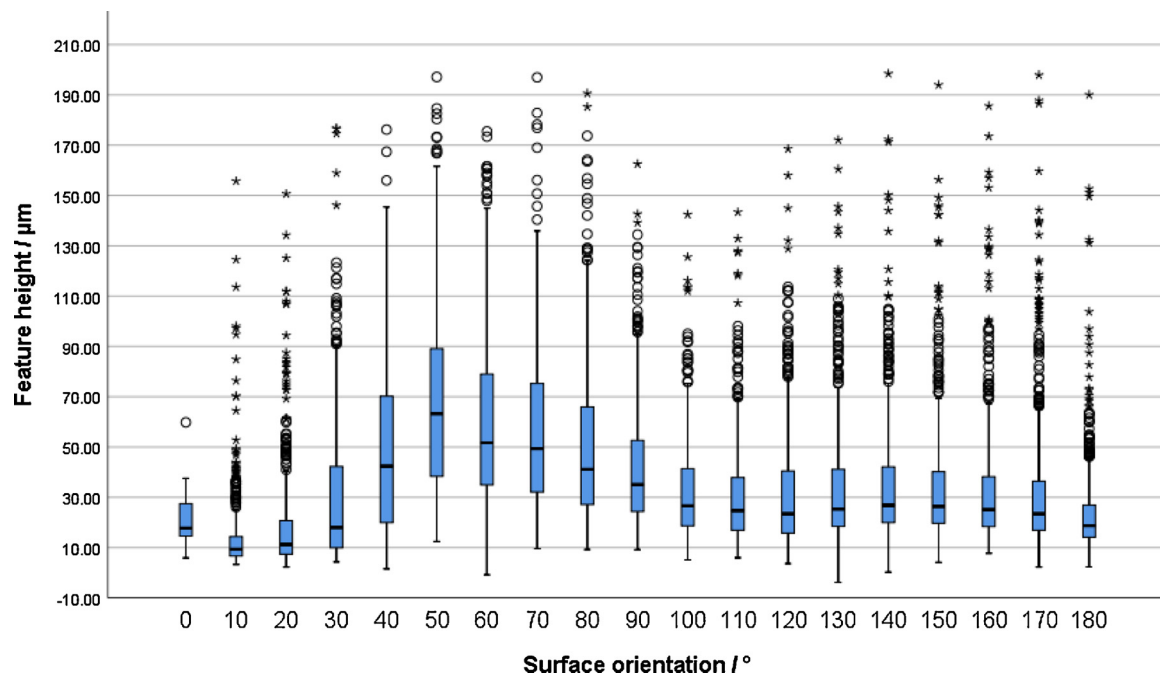


Fig. 8. Feature height (height of the individual feature with respect to its surroundings) as a function of surface orientation. Median, interquartile range (IQR), whiskers (approx. 95 % of the data) and outliers are shown (circles denote outliers; asterisks denote extreme outliers greater than three times the IQR).

there is an increase in the dispersion of the results, which may be attributed to the increased difficulty encountered by the segmentation approach in defining the feature boundaries. In fact, at these orientations, there is an increasing number of features appearing in clustered form. The additional presence of the staircase effect creates additional protruded formations that are often mistaken as features by the method.

The behaviour of the feature height attribute (height of the individual features, as defined in Section 2.4), is illustrated in Fig. 8. Feature height increases with orientation up to 50°, after which the indicator decreases until reaching a plateau for orientations greater than 100°. An explanation for the initial increase of feature height could be the staircase effect confusing the segmentation algorithm: the border of each layer creates a protruded ridge, very well visible on the surface and of height comparable or superior to that of particles and spatter. The segmentation method is therefore tricked into falsely identifying the ridges as if they were large agglomerates of particles thus leading to biased estimations of feature attributes, including feature height. The dispersion of the indicator decreases for orientations greater than 90°.

Feature area, defined in Section 2.4 as the area of a topologically isolated feature, is plotted against surface orientation in Fig. 9. Increment of average area are to be considered caused by two phenomena: the increment of clustering effects (leading the method to assigning a larger area to an individual feature) and the presence of the staircase effect (leading the method to mistakenly consider larger ridges as features).

Finally, feature coverage (the ratio of the total area covered by the features and the entire measured area, as defined in Section 2.4) is shown in Fig. 10. Note that there is only one value of the feature coverage indicator per each region. As three regions were measured per orientation, each boxplot in Fig. 10 is generated using three data points. From looking at Fig. 10, for the 0° orientation surface there is almost no feature coverage, as expected from the very small feature count. The indicator value increases up to the 80° orientation. The scatter of indicator values across the three regions of each surface (hinted at by the length of each boxplot) is rather small for most surface orientations with exception for those between 80° to 110°. These latter surfaces also possess a larger dispersion for feature count.

3.2. Characterisation based on ISO 25178 – 2 texture parameters

Texture parameters were computed both on the original topographies (topographies as-measured) and on the feature-deprived ones (topographies subject to the removal of points identified as features), as illustrated in Section 2.4. In the following the feature-deprived topographies are referred to as “feature-deprived” surfaces, whilst the original ones are referred to as “original topography” surfaces. Texture parameters were computed for each measurement from three surface regions for each individual orientation in the test part, leading to a total of three observations for each parameter for each surface case.

The texture parameters S_a and S_q are reported in Figs. 11 and 12. Both show an oscillating pattern with respect to surface orientation, with the parameter value generally increasing up to the 70° orientation, decreasing to the 110° orientation, increasing again until the 150° orientation then decreasing again. The parameters S_a and S_q both capture the vertical dispersion of surface height values with respect to a virtual mean plane; the higher the parameter, the higher the dispersion (i.e. the “rougher” the surface). The feature-deprived surfaces present slightly smaller parameter values, consistent with the removal of protruded features thus leading to a general decrease of dispersion. There is an increased dispersion of parameter values across the three regions when considering the feature-deprived surfaces between orientations of 50° and 100°. This may be due to the increased prevalence of agglomerations of particles creating errors in the segmentation, and to the increased presence of protruded ridges further confusing the segmentation. A less consistent performance in feature-removal leads to sparser values for the texture parameters computed on the feature-deprived surface. A similar dispersion of parameter values is also observed for the surfaces at orientations between 130° and 160° (downward facing).

The texture parameter S_z captures the extremes of the range of height values of a surface (the larger S_z , the more different the local maximum and minimum heights of a surface). Despite not being particularly reliable (being influenced even by the smallest peak or pit) S_z is still popular and widely reported in surface characterisation protocols. The values of S_z as a function of surface orientation are shown in Fig. 13. As for the other texture parameters, there are three values per orientation, corresponding to the values computed on the three

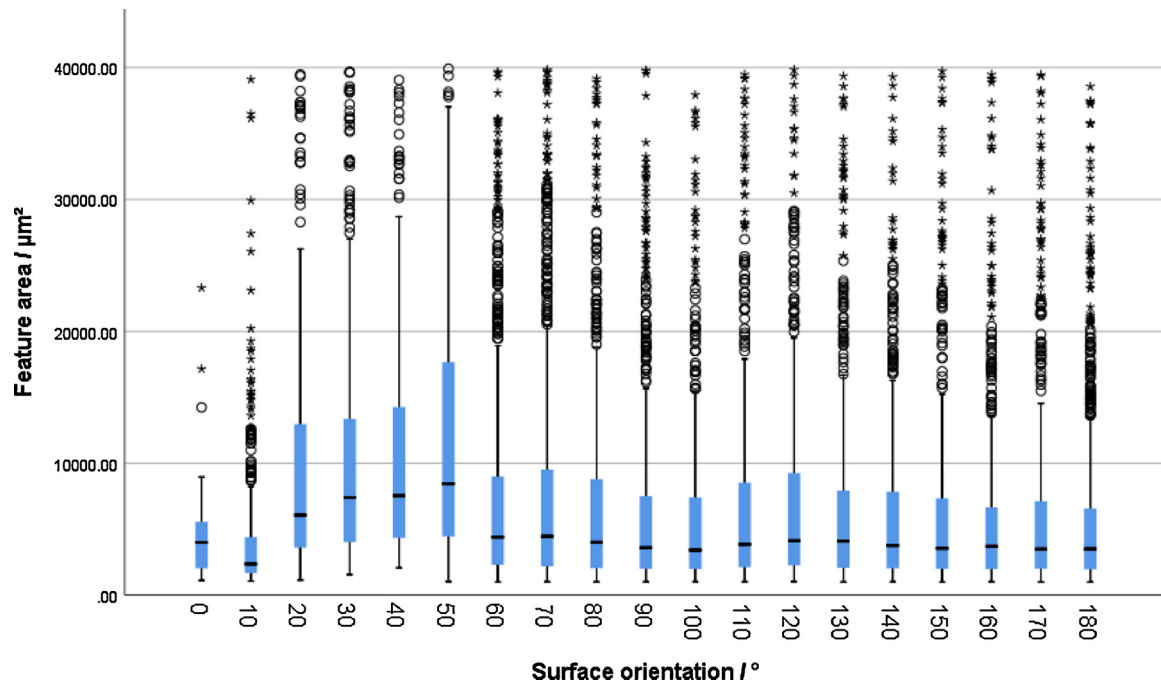


Fig. 9. feature area (area of the individual feature) as a function of surface orientation. Median, interquartile range (IQR), whiskers (approx. 95 % of the data) and outliers are shown (circles denote outliers; asterisks denote extreme outliers greater than three times the IQR).

sampled regions. By observing Fig. 13, the S_z parameter appears to increase with orientation, whilst there is often a reduction of value for S_z in the feature-deprived surface with respect to the original one, which is consistent with removing the particle/spatter features, expected to cause a reduction of height ranges. However, because S_z is affected by singularities, a higher likelihood should be considered of events where segmentation error may lead to leftovers (i.e. portions of feature “walls” left in the topography after feature removal) influencing the final value of the texture parameter and thus contributing to increasing the dispersion of the parameter values. The dispersion of S_z across the three regions for each surface orientation seems to match the

behaviour observed for S_a and S_q , with a large dispersion affecting in particular the original topography between 130° and 160°, and the orientations between 50° and 100° for the feature-deprived surfaces, again possibly due to segmentation errors affecting the results.

The behaviours of the surface texture parameters skewness (S_{sk}) and kurtosis (S_k) are shown in Fig. 14 and Fig. 15. Again, three values are available from the three regions sampled at each surface orientation. The S_{sk} and S_k parameters characterise the shape of the probability distribution of height values of the topography with respect to a reference mean plane. Skewness is a measure of symmetry of the distribution around the mean plane (it is the third-order moment of the

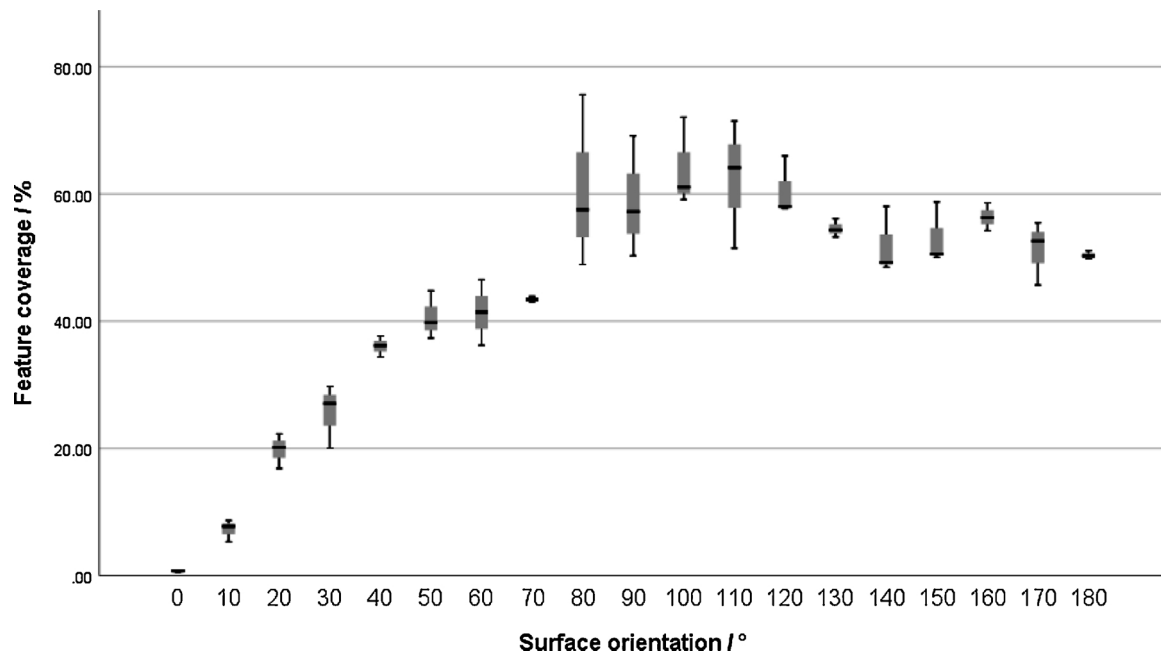


Fig. 10. Feature coverage (ratio of the total area occupied by features and the entire measured area) as a function of surface orientation. Median, interquartile range (IQR) and whiskers.

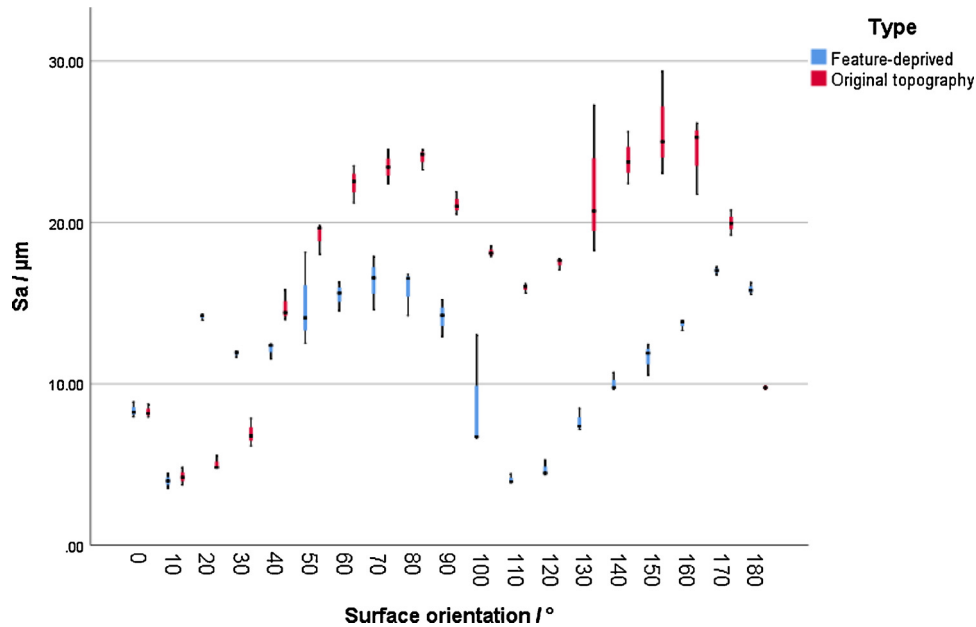


Fig. 11. Surface texture parameter S_a for feature-deprived topography (blue) and original topography (red) with respect to surface orientation. Median, interquartile range (IQR) and whiskers.

distribution). Ssk indicates whether heights are preferentially distributed above (negative Ssk) or below (positive Ssk) the mean plane. In Fig. 14 the Ssk parameter decreases from 20° to 100° orientation, then slightly increases after 110° . The feature-deprived surfaces tend to have lower Ssk because of the removal of height content above the mean height plane (i.e. particle and spatter features).

Kurtosis is the fourth-order moment of the probability distribution of heights. It indicates whether the distribution has a spiky shape ($Sk_u > 3$) or whether on the contrary it is low and widespread ($Sk_u < 3$), the shape of a Gaussian distribution being represented as $Sk_u = 3$. In Fig. 15, Sk_u is greater than 3 for all surfaces, but feature-deprived surfaces have generally smaller Sk_u values, which is again consistent with the removal of extremal height values above the mean height plane. The large dispersions observed for Sk_u at the 0° and 180° cases deserves further investigation.

4. Discussion

Feature-based characterisation approaches provide an alternative and complementary characterisation route to conventional texture parameters for the assessment of surface topography. Feature-based characterisation pursues the investigation of individual topographic formations of interest, of relevance to the specific application. Whilst texture parameters are exclusively dependent on the statistical properties of the topography dataset, feature-based characterisation implies that application-related knowledge is inserted in the characterisation process, and custom data processing pipelines must be implemented to identify and extract the relevant features.

Because of the need for application-specific knowledge, feature-based characterisation is often referred to as an information-rich

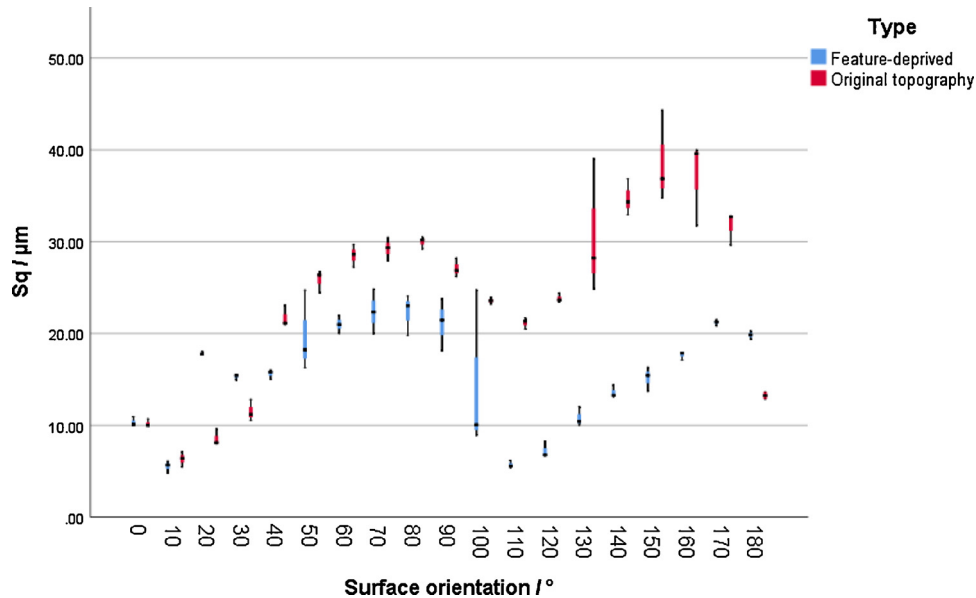


Fig. 12. Surface texture parameter S_q for feature-deprived topography (blue) and original topography (red) with respect to surface orientation. Median, interquartile range (IQR) and whiskers.

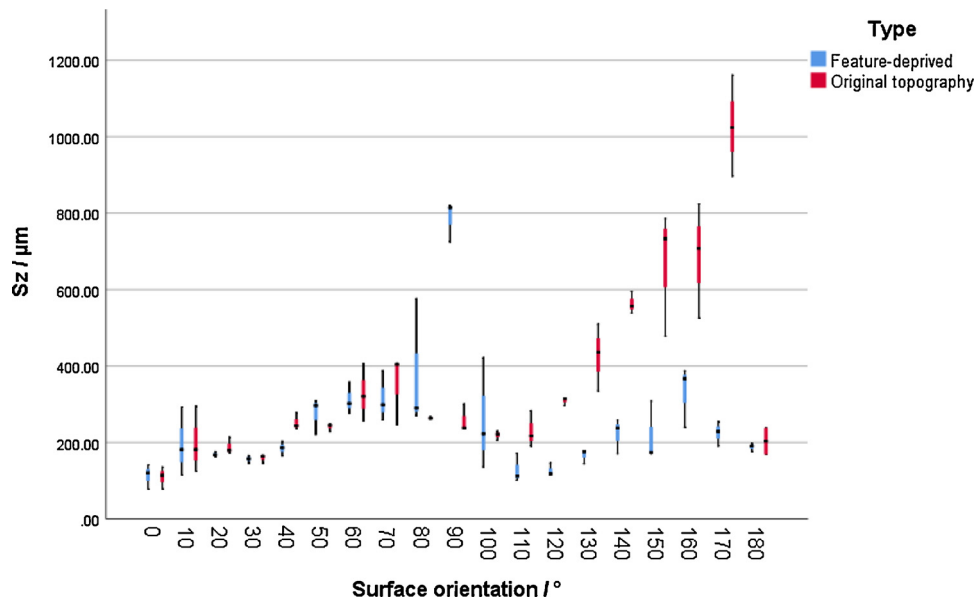


Fig. 13. Surface texture parameter S_z for feature-deprived topography (blue) and original topography (red) with respect to surface orientation. Median, interquartile range (IQR) and whiskers.

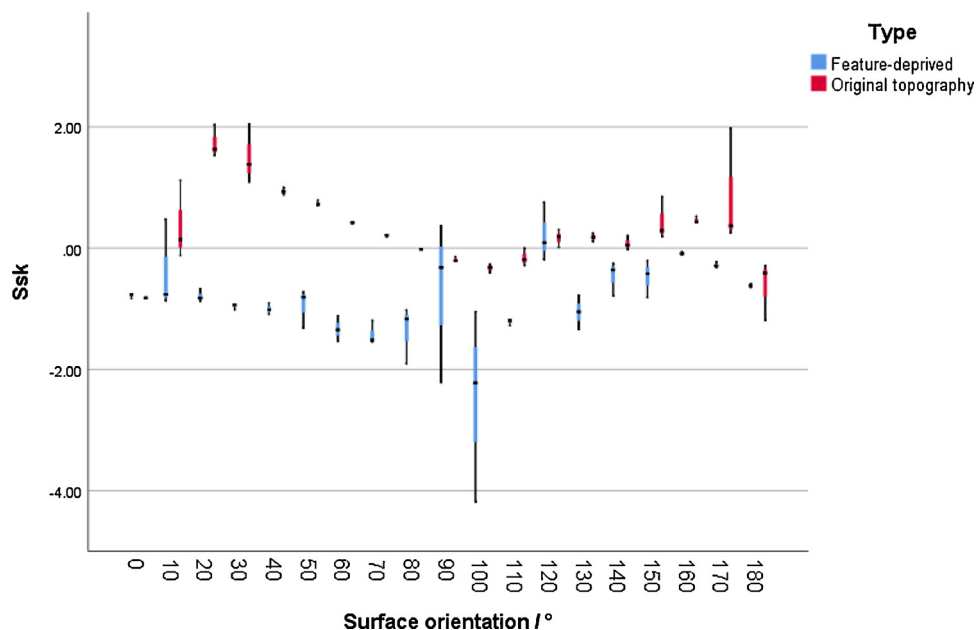


Fig. 14. Surface texture parameter S_{sk} for feature-deprived topography (blue) and original topography (red) with respect to surface orientation. Median, interquartile range (IQR) and whiskers.

approach to the characterisation of surfaces [33]. The added characterisation effort is generally compensated by the possibility of delving deeper into the investigation of a surface, targeting elements that are of more direct interest to the application. For AM surfaces for example, this means providing quantitative data that may help researchers better observe the surface, and thus more effectively explore the physics of the manufacturing process, possibly also identifying more informative links between manufacturing process parameters and resulting topography. For example, the focus on spatter formations and particles shown in this work drove the development of a feature-based characterisation pipeline where such features can be identified and quantified. This pipeline now can be offered as a new observational tool for researchers to investigate how spatter and particles are related to controllable manufacturing process parameters, for example, in this case, surface orientation with respect to the build direction. Moreover, feature-based

characterisation offers the possibility for the surface to be decomposed, for example by elimination of identified features. In this case, it is thus possible to obtain a feature-deprived topography that can still be characterised in terms of conventional texture parameters.

The complications and limitations with feature-based approaches are on how to communicate and document the resulting information. Concepts such as feature count, feature height, feature area, etc. are not necessarily straightforward, and imply additional efforts to reach to a shared agreement on definitions and procedures to compute the related quantitative indicators. Whilst the computation of universal texture parameters such as S_a or S_q (or the others shown in this work) implies conformance to simple, existing, specified protocols defined in international standards and that anyone could reproduce (implying that texture parameter results may be easily comparable across operators as long as the protocols are respected), feature-based characterisation

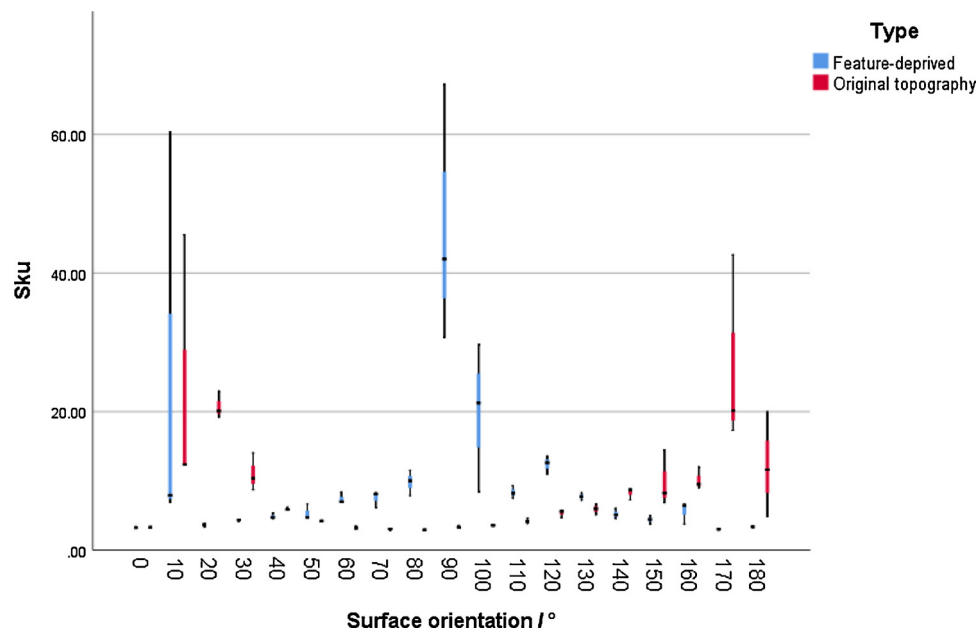


Fig. 15. Surface texture parameter Sku for feature-deprived topography (blue) and original topography (red) with respect to surface orientation. Median, interquartile range (IQR) and whiskers.

protocols are more difficult to share, given their increased dependence on surface type and application context. Operators must always make considerations on how they define a feature within the topography, ensuring that the segmentation approach meaningfully determines the boundaries of these features. The dimensional assessment of feature coverage and other attributes of the features also require definition, to ensure that meaningful parameters can be extracted and compared.

It must be clarified that feature-based characterisation, as well as hybrid approaches combining feature-based characterisation with conventional characterisation based on texture parameters, do not directly solve manufacturing research problems, but do provide new observational viewpoints, i.e. novel perspectives which can help solving manufacturing research problems. Thus, whilst feature-based characterisation approaches do not replace the research work needed to understand the physics of a manufacturing process, or the relationships between controllable process parameters and observed results, they do indeed provide potentially useful, new quantitative information which would not be available before. In this work, for example, it was shown that it is now possible to quantify particle/spatter count, spatial distribution and geometrical properties, providing a series of new quantitative indicators useful to investigate EBPBF surfaces. In this work the investigation has been based on looking at surface orientation, in future works other controllable parameters may be explored.

Whilst it is not within the scope of this work to directly collate feature-based characterisation to aspects of the manufacturing process, what can be inferred here is that there are clearer correlations between surface orientation and feature-based indicators targeting particles/spatter, in particular if compared to observable correlations between orientation and texture parameters. Clearly, if it is assumed that particles adhere to EBPBF surfaces in different amounts and with different aggregation behaviour depending on orientation, then there is no conventional texture parameter explicitly describing particle-related properties, hence the better result using dedicated (i.e. feature-based) indicators.

Finally, a richer depiction of surface topography as achievable by adding feature-based characterisation to conventional (parameter based) characterisation results, clearly provides new information for planning the surface finishing process, an essential aspect of industrial production by additive manufacturing. For example, instead of simply saying if a surface is rougher than another, dedicated feature-based

approaches can provide hints that in some cases the dominant contribution to roughness is due to attached particles (versus irregularity of the substrate in other cases) thus leading to the implementation of more optimised, or surface-specific methods for performing finishing operations.

5. Conclusions

Feature-based characterisation has been used in this work to identify spatter and particles on EBPBF surfaces, with the purpose of studying how topographies vary as a function of surface orientation with respect to the build angle. The results indicate how feature-based characterisation can be useful at describing topographies providing additional perspectives on the surface, possibly useful better support research in understanding the events underlying a manufacturing process, and the relationships between controllable process parameters and produced surface topography. It has been also shown how feature-based characterisation can be used in combination to conventional characterisation via texture parameters, for example allowing the characterisation of the surface substrate once particles and spatter have been removed. This approach can also provide new perspectives to analyse surface topography, as it can be used to produce texture parameter values without the influence of unwanted features.

CRediT authorship contribution statement

Lewis Newton: Conceptualization, Methodology, Software, Validation, Formal analysis, Investigation, Data curation, Writing - original draft, Writing - review & editing, Visualization, Project administration. **Nicola Senin:** Conceptualization, Methodology, Software, Validation, Resources, Data curation, Writing - review & editing, Supervision. **Evangelos Chatzivagiannis:** Resources, Writing - review & editing, Supervision. **Bethan Smith:** Resources, Supervision, Funding acquisition. **Richard Leach:** Conceptualization, Resources, Writing - review & editing, Supervision, Project administration, Funding acquisition.

Declaration of Competing Interest

The authors declare that they have no known competing financial interests or personal relationships that could have appeared to influence the work reported in this paper.

Acknowledgements

We would like to thank the Engineering and Physical Sciences Research Council (Grants EP/L01534X/1 and EP/M008983/1) and Charlie McGuinness of the Manufacturing Technology Centre (Coventry, UK) for help in generating the EBPBF samples.

References

- [1] I. Gibson, D. Rosen, B. Stucker, *Additive Manufacturing Technologies*, Springer New York, New York, NY, 2015, <https://doi.org/10.1007/978-1-4939-2113-3>.
- [2] Z. Chen, X. Wu, D. Tomus, C.H.J. Davies, Surface roughness of selective laser melted Ti-6Al-4V alloy components, *Addit. Manuf.* 21 (2018) 91–103, <https://doi.org/10.1016/j.addma.2018.02.009>.
- [3] A. Kudzal, B. McWilliams, C. Hofmeister, F. Kellogg, J. Yu, J. Taggart-Scarff, J. Liang, Effect of scan pattern on the microstructure and mechanical properties of Powder Bed Fusion additive manufactured 17-4 stainless steel, *Mater. Des.* 133 (2017) 205–215, <https://doi.org/10.1016/j.matdes.2017.07.047>.
- [4] M. Jamshidinia, R. Kovacevic, The influence of heat accumulation on the surface roughness in powder-bed additive manufacturing, *Surf. Topogr. Metrol. Prop.* 3 (2015), <https://doi.org/10.1088/2051-672X/3/1/014003>.
- [5] N. Senin, A. Thompson, R. Leach, Feature-based characterisation of signature topography in laser powder bed fusion of metals, *Meas. Sci. Technol.* 29 (2018) 045009, <https://doi.org/10.1088/1361-6501/aa9e19>.
- [6] C. Körner, Additive manufacturing of metallic components by selective electron beam melting — a review, *Int. Mater. Rev.* 61 (2016) 361–377, <https://doi.org/10.1080/09506608.2016.1176289>.
- [7] A. Townsend, N. Senin, L. Blunt, R.K. Leach, J.S. Taylor, Surface texture metrology for metal additive manufacturing: a review, *Precis. Eng.* 46 (2016) 34–47, <https://doi.org/10.1016/j.precisioneng.2016.06.001>.
- [8] ISO 4287, Geometrical Product Specification (GPS) - Surface Texture: Profile Method - Terms, Definitions and Surface Texture Parameters, (2009), <https://doi.org/10.3403/02031657>.
- [9] G. Strano, L. Hao, R.M. Everson, K.E. Evans, Surface roughness analysis, modelling and prediction in selective laser melting, *J. Mater. Process. Technol.* 213 (2013) 589–597, <https://doi.org/10.1016/j.jmatprotec.2012.11.011>.
- [10] K. Mumtaz, N. Hopkinson, K. Mumtaz, N. Hopkinson, Top Surface and Side Roughness of Inconel 625 Parts Processed Using Selective Laser Melting, (2009), <https://doi.org/10.1108/13552540910943397>.
- [11] A. Boschetto, L. Bottini, F. Veniali, Roughness modeling of AlSi10Mg parts fabricated by Selective Laser Melting *Journal of Materials Processing Technology Roughness modeling of AlSi10Mg parts fabricated by selective laser melting*, *J. Mater. Process. Tech.* 241 (2018) 154–163, <https://doi.org/10.1016/j.jmatprotec.2016.11.013>.
- [12] ISO 25178-2:2012, Geometrical Product Specifications (GPS) - Surface Texture: Areal - Part 2: Terms, Definitions and Surface Texture Parameters, (2012).
- [13] T. Grimm, G. Wiora, G. Witt, Characterization of typical surface effects in additive manufacturing with confocal microscopy, *Surf. Topogr. Metrol. Prop.* 3 (2015), <https://doi.org/10.1088/2051-672X/3/1/014001>.
- [14] A.T. Sidambe, Three dimensional surface topography characterization of the electron beam melted Ti6Al4V, *Met. Powder Rep.* 72 (2017) 200–205, <https://doi.org/10.1016/j.mprp.2017.02.003>.
- [15] J.C. Fox, S.P. Moylan, B.M. Lane, Effect of process parameters on the surface roughness of overhanging structures in laser powder bed Fusion additive manufacturing, *Procedia Cirp* 45 (2016) 131–134, <https://doi.org/10.1016/j.procir.2016.02.347>.
- [16] A. Triantaphyllou, C.L. Giusca, G.D. Macaulay, F. Roerig, M. Hoebel, R.K. Leach, B. Tomita, K.A. Milne, Surface texture measurement for additive manufacturing, *Surf. Topogr. Metrol. Prop.* 3 (2015) 024002, <https://doi.org/10.1088/2051-672X/3/2/024002>.
- [17] N. Senin, L. Blunt, Characterisation of individual areal features, in: R.K. Leach (Ed.), *Characterisation Areal Surf. Texture*, Berlin, Heidelberg, 2013, pp. 179–216.
- [18] S. Lou, X. Jiang, W. Sun, W. Zeng, L. Pagani, P.J. Scott, Characterisation methods for powder bed fusion processed surface topography, *Precis. Eng.* 57 (2019) 1–15, <https://doi.org/10.1016/j.precisioneng.2018.09.007>.
- [19] A.V. Krishna, O. Flys, V.V. Reddy, A. Leicht, L. Hammar, B. Rosen, Potential approach towards effective topography characterization of 316L stainless steel components produced by selective laser melting process, *Proc. 18th Int. Euspen Conf., Venice, Italy* (2018) Jun.
- [20] L. Newton, N. Senin, B. Smith, R. Leach, Feature-based characterisation of evolving surface topographies in finishing operations for additive manufacturing, *Proc. 18th Int. Euspen Conf., Venice, Italy*, (2018) Jun.
- [21] L. Newton, N. Senin, B. Smith, E. Chatzivagiannis, R.K. Leach, Comparison and validation of topography segmentation methods for feature-based characterisation of metal powder bed fusion surfaces, *Surf. Topogr. Metrol. Prop.* Submitted (2019).
- [22] ISO 25178-2:2012, Geometrical Product Specification (GPS) — Surface Texture: Areal Part 606 : Nominal Characteristics of Non-contact (focus Variation) Instruments, (2015).
- [23] L. Newton, N. Senin, C. Gomez, R. Danzl, F. Helml, L. Blunt, R. Leach, Areal topography measurement of metal additive surfaces using focus variation microscopy, *Addit. Manuf.* 25 (2019) 365–389, <https://doi.org/10.1016/j.addma.2018.11.013>.
- [24] G.D. MacAulay, N. Senin, C.L. Giusca, R.K. Leach, A. Ivanov, Review of feature boundary identification techniques for the characterization of tessellated surfaces, *Surf. Topogr. Metrol. Prop.* 3 (2015), <https://doi.org/10.1088/2051-672X/3/1/013002>.
- [25] C. Vicent, K. Ron, S. Guillermo, Geodesic active contours, *Int. J. Comput. Vis.* 22 (1997) 61–79.
- [26] R.T. Whitaker, A level-set approach to 3D reconstruction from range data, *Int. J. Comput. Vis.* 29 (1998) 203–231, <https://doi.org/10.1023/A:1008036829907>.
- [27] R.C. Gonzales, R.E. Woods, *Digital Image Processing*, 4th ed., Pearson, New York, NY, 2018.
- [28] H. Zhu, *Measurement and Characterisation of micro/nano Scale Structured Surfaces* (Thesis) University of Huddersfield, (2012).
- [29] A.B. Forbes, Areal form removal, in: R.K. Leach (Ed.), *Characterisation Areal Surf. Texture*, Springer, Berlin Heidelberg, Berlin Heidelberg, 2013, pp. 107–128, <https://doi.org/10.1007/978-3-642-36458-7>.
- [30] S. Vock, B. Klöden, A. Kirchner, T. Weißgärber, B. Kieback, Powders for powder bed fusion: a review, *Prog. Addit. Manuf.* 0 (2019), <https://doi.org/10.1007/s40964-019-00078-6>.
- [31] Digital Surf, Mountains® Surface Imaging & Metrology Software, [Digitalsurf.Com/](http://www.digitalsurf.com/), (2018) <http://www.digitalsurf.com/en/mntkey.html>.
- [32] M.F. Zäh, S. Lutzmann, Modelling and simulation of electron beam melting, *Prod. Eng.* 4 (2010) 15–23, <https://doi.org/10.1007/s11740-009-0197-6>.
- [33] N. Senin, R. Leach, Information-rich surface metrology, *Procedia Cirp* 75 (2018) 19–26, <https://doi.org/10.1016/j.procir.2018.05.003>.